Indonesian Physical Review
Volume 08 Issue 01, January 2025
P-ISSN: 2615-1278, E-ISSN: 2614-7904

The Application of Plastic Fiber Optic Sensor as Blood Pressure Monitoring Sensor

Fadli Ama[1,2], Agus Muhamad Hatta[1]*, Katherin Indriawati[1], Frans R. Agustiyanto[1,3], Shofi Afghania Usamah[4], Alfian Pramudita Putra[2], Sigit Dani Perkasa[5]

[1] *Department of Physical Engineering, Faculty of Industrial Technology and Systems Engineering, Institut Teknologi Sepuluh Nopember (ITS), Surabaya 60111, Indonesia*
[2] *Biomedical Engineering Study Program, Department of Physics, Faculty of Science and Technology, Universitas Airlangga (UNAIR), Surabaya 60115, Indonesia*
[3] *Department of Physics, Faculty of Tarbiyah and Educational Science, Universitas Islam Negeri (UIN) Mahmud Yunus Batusangkar, Sumatera Barat 27213, Indonesia*
[4] *Biomedical Engineering Master Program Study, Faculty of Science and Technology, Universitas Airangga, Surabaya, Indonesia*
[5] *Electrical Engineering Study Program, Department of Engineering, Faculty of Advanced Technology and Multidiscipline, Universitas Airlangga (UNAIR), Surabaya 60115, Indonesia*

*****Corresponding Authors E-mail: amhatta@ep.its.ac.id*

Article Info

Article info:
Received: 17-09-2024
Revised: 22-01-2025
Accepted: 23-01-2025

Keywords:
Blood Pressure; Pulse Transit Time; Cuffless Design; Configuration Sensor; Tapered PFOS

How To Cite:
F. Ama, A. M. Hatta, K. Indriawati, F. R. Agustiyanto, S. A. Usamah, A. P. Putra, S. D. Perkasa, "The application of fiber optic sensor as a blood pressure monitoring", Indonesian Physical Review, vol. 8, no. 1, p 300-314, 2025.

DOI:
https://doi.org/10.29303/ipr.v8i1.395

Abstract

Continuous blood pressure monitoring is essential for early hypertension prevention and cardiovascular disease diagnosis. Traditional methods are unsuitable for long-term use due to discomfort and limited portability. This study presents a tapered plastic fiber optical sensor (PFOS) as a sustainable, non-invasive solution for continuous monitoring. The PFOS system employs a light modulator based on mechanical waves to detect arterial pressure changes, utilizing an infrared light source (940 nm). The cuffless design includes four configurations: Bend, Bend with 1 Scratch, Bend with 3 Scratches, and Straight with 3 Scratches. The Bend with 1 Scratch configuration demonstrated superior performance, achieving 99.84% accuracy, a mean absolute error (MAE) of 0.1564, a linearity of 0.9999, and a sensitivity of 2.9997 Hz/dBm. Experimental validation involved testing radial and brachial arteries. Blood pressure estimates from Pulse Transit Time (PTT) were compared to a standard sphygmomanometer. On the radial artery, the Bend with 1 Scratch configuration achieved the best results, with the lowest MAE (1.72 for SBP, 2.39 for DBP) and highest accuracy (98.30% for SBP, 96.56% for DBP). On the brachial artery, the Straight with 3 Scratches configuration performed best, with an MAE of 2.81 for SBP and 5.11 for DBP and accuracies of 97.21% for SBP and 92.67% for DBP. The PFOS system offers a promising option for continuous monitoring in clinical and home settings.

Introduction

Blood pressure is a significant global health issue and is considered a symptom of diseases such as hypertension [1], [2], stroke [3], and cardiovascular diseases (CVD) [4]. Hypertension, or high blood pressure, is characterized by systolic blood pressure above 140 mmHg and diastolic blood pressure exceeding 90 mmHg in two measurements taken five minutes apart while the individual is relaxed [5]. The American Heart Association [6] also notes several factors influencing systolic blood pressure (SBP) and diastolic blood pressure (DBP), including age, gender, body mass index, psychological and medical conditions, genetics, and lifestyle. According to the World Health Organization [7], in 2015, approximately 1.13 billion people worldwide were diagnosed with hypertension, with projections increasing to 1.5 billion by 2025, causing 9.4 million deaths annually due to its complications [8]. Hypertension is known as The Silent Killer, as it can lead to permanent disability and sudden death [29], with a prevalence in Indonesia reaching 34.1% in 2019, up from 25.8% in 2013 [8], [29]. WHO reported in 2023 that 1.28 billion adults aged 30-79 suffer from hypertension, with 46% unaware of their condition, resulting in inadequate treatment and potential target organ damage depending on the duration and severity of undetected and untreated high blood pressure [7]. Therefore, it is important to be aware of blood pressure conditions as early as possible and to conduct accurate diagnoses to prevent adverse effects in the future, as shown in Figure 1.

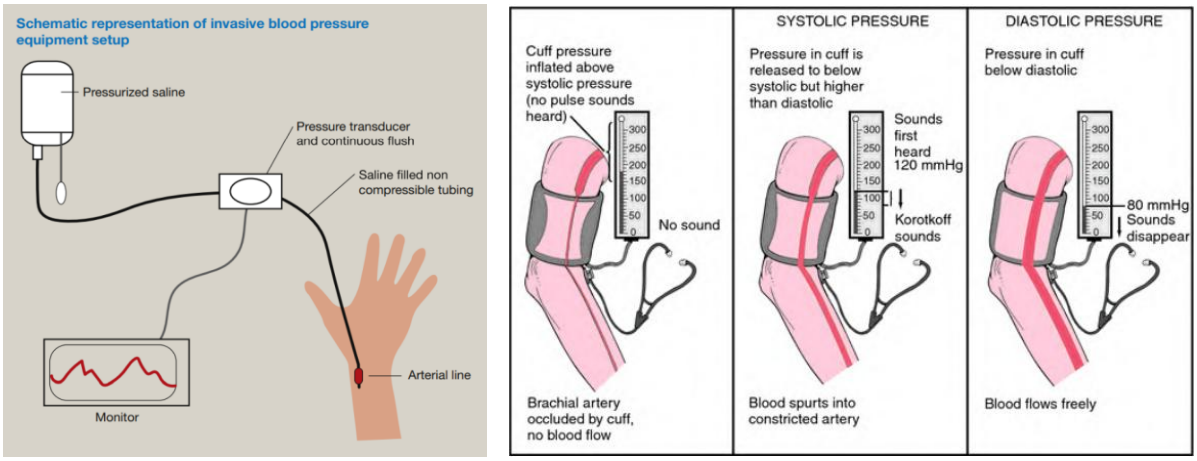

(a) (b)

Figure 1. Blood pressure measurement method: (a) Invasive, (b) non-invasive [9][10]

The blood pressure measurement methods shown in Figure 1 are divided into two categories: invasive and non-invasive [9], [10]. The invasive method involves inserting a transducer into the peripheral artery, providing accurate results but causing pain and discomfort for the patient. Conversely, the non-invasive method, where the transducer cuff is placed at the brachial artery using Oscillo-metric [11], auscultatory [12], and ultrasonographic methods [30]. The easiest method to extract blood pressure according to the literature is pulse arrival time (PAT) [14], pulse transit time (PTT) [13], [14], [15], and pulse wave analysis (PWA)[16]. The blood pressure measurement commonly used by doctors is non-invasive, as shown in Figure 1(b), performed at the brachial artery with inflatable cuff technology, using the Korotkoff sound or Oscillo-metric method. Conventional blood pressure measurement using inflatable cuff technology is often uncomfortable [17] and has many drawbacks, such as inappropriate cuff size, repeated inflation causing discomfort, complicated operation, and requiring the

patient to remain still [18]. Additionally, current commercial blood pressure measurement is unsuitable for continuous monitoring due to the physical limitations of the devices.

Many researchers are developing optical fiber sensors for blood pressure measurement to address this issue. Optical sensors have advantages such as high stability against temperature, pressure, and humidity changes, as well as high accuracy and resistance to electromagnetic interference [19]. Plastic optical fiber sensors offer higher flexibility and resistance to bending compared to silica-FBG sensors [20], [21]. Previous studies have shown that vital signs of blood pressure can be identified using pulse wave signals measured with silica-FBG optical fiber sensors, although silica optical fibers are brittle and hazardous when broken [22]. Plastic optical fiber sensors of the FBG type are safer and more flexible, and do not produce sharp edges when broken [23]. Heart rate measurements using POF-FBG in the brachial artery showed a 20-fold increase in sensitivity compared to silica-FBG sensors [24]. The development of sensors for blood pressure monitoring using a Pulse Transit Time (PTT) blood pressure estimation model with data from 45 subjects showed systolic blood pressure (SBP) errors of 0.24 ± 2.39 mmHg and diastolic blood pressure (DBP) errors of 0.12 ± 2.62 mmHg, but further research is needed to address noise caused by body movements [17].

This study aims to develop a blood pressure measurement system using plastic optical fiber (POF) sensors that can be used for cardiovascular system monitoring and early prevention of hypertension. This sensor is expected to provide more comfort compared to conventional sphygmomanometers and be safer than silica optical fiber-based blood pressure sensors. Blood pressure measurement will be conducted using the Pulse Transit Time (PTT) method, by testing various plastic optical fiber configurations and sensor placement positions on the body. The performance of the sensor will be evaluated based on accuracy using the Mean Absolute Error (MAE) parameter. The use of optical fiber sensors offers advantages in terms of accuracy and sensitivity to changes.

Methodology

Arterial Pulse Wave

Arterial pulse waves are waves generated by the contraction and relaxation of the heart as they pump blood into the arteries. The wave in Figure 2(a) reflects changes in arterial pressure during the cardiac cycle, starting from the maximum pressure during contraction (proximal part) to the minimum pressure when the heart relaxes (distal part). The arterial pulse wave is a response to the heart's contraction impulses that cause a surge in arterial pressure. The peak of the arterial pulse wave reflects systolic pressure, while the lowest point reflects diastolic pressure.

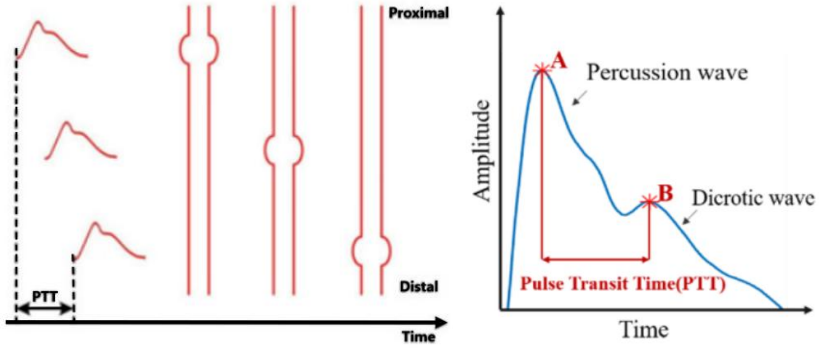

(a) (b)

Figure 2. Arterial pulse wave with pulse transit time (PTT) [17]

The wave in Figure 2(b) consists of two main peaks, namely the percussion wave and the dicrotic wave. The percussion wave occurs when the heart's ventricles contract and pump blood into the aorta, causing the arteries to expand and produce systolic pressure. After that, when the aortic valve closes, blood flows back from the arteries to the ventricles, forming the dicrotic wave14. Pulse Transit Time (PTT) is the time it takes for a pulse wave to travel from one point in the cardiovascular system to another. Specifically, PTT measures the time required for the pulse wave to move from the heartbeat to reach a certain point in the artery, from the peak of the percussion wave to the peak of the dicrotic wave. PTT is an important indicator in blood pressure analysis, where the transit time of the pulse wave can be used to estimate blood pressure. Increased blood pressure usually speeds up PTT because of the faster pulse wave velocity in stiffer arteries. Conversely, decreased blood pressure slows down PTT.

Sensor Design

This study uses plastic optical fibers with a multimode step-index structure developed through the macro-bending method to enhance the sensitivity and responsiveness of the sensor through physical manipulation of the plastic optical fiber, where the effectiveness of small changes in the curvature of the optical fiber results in significant changes in the transmission power of blood pressure in the arteries. This study uses four variations of the sensing area, namely Bend configuration, Bend with 1 Scratch, Bend with 3 Scratches, and Straight with 3 Scratches. In each sensor configuration shown in Figure 3, the jacket structure was removed over a length of 3 cm using a stripper, and the cladding was cleaned using acetone. This length is adjusted to the pulse area in the brachial artery and radial artery for sensor sensing area placement on the body. This approach aims to address technical challenges associated with the use of optical fibers, such as power loss due to bending or stretching. As demonstrated in previous research [17]. The primary objective of these configuration variations is to identify the optimal configuration that provides the best sensitivity and accuracy in detecting blood pressure, while ensuring consistency of results across different measurement sites.

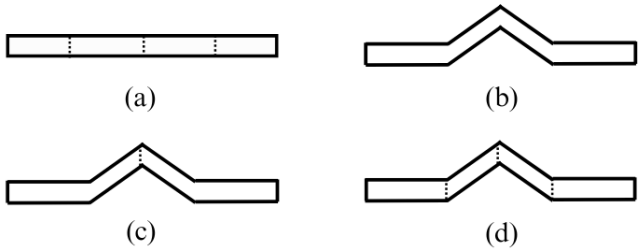

Figure 3. Blood pressure measurement sensor configuration design (a) Straight 3 Scratches (b) Bend (c) Bend 1 Scratch (d) Bend 3 Scratches

In Figure 3(b) The sensing area on the sensor with a bend configuration is divided into three bend angles to increase sensitivity to changes in blood pressure. In Figure 3(c) and Figure 3(d), the sensor with a bending configuration with scratches is bent and scratched in the sensing area, while in Figure 3(a) This sensor configuration uses optical fibers laid in a straight line with three scratches along the fiber.

Sensor Calibration

This study uses an infrared light source with a wavelength of 940 nm and polymethyl methacrylate (PMMA) plastic, which has a good absorption profile at wavelengths around 940 nm and good transparency, allowing infrared light to propagate with minimal attenuation. This is consistent with other studies that used a light source with a wavelength of 950 nm for plastic optical fiber sensors [20], [23]. The sensor configuration setup used in this study is illustrated by the block diagram in Figure 4.

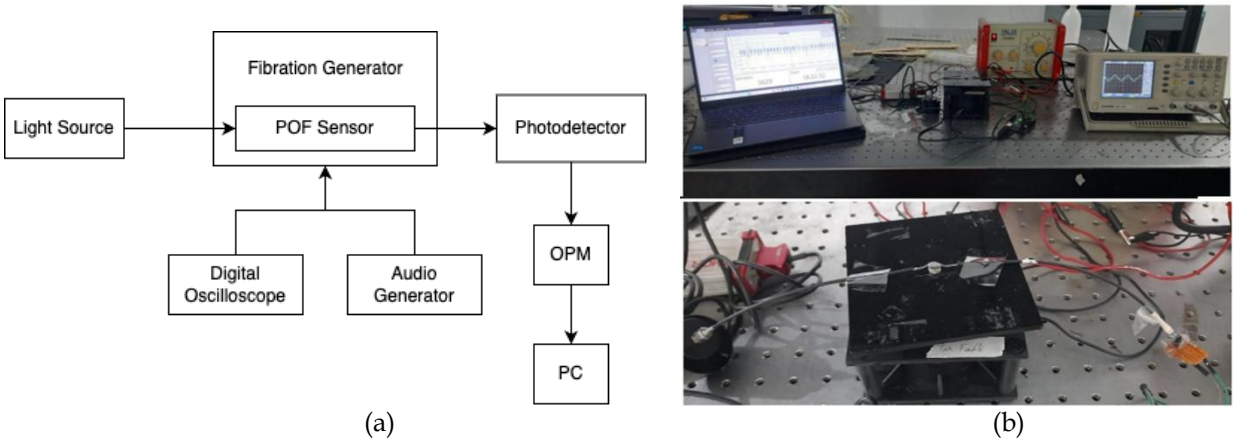

Figure 4. Sensor calibration setup: (a) block diagram; (b) sensor design trial in photonic laboratory

In Figure 4, the designed sensor is connected to a light source in the form of an LED and a microcontroller at one end, and an optical power meter (OPM) at the other end, which is then connected to a PC for data processing. The sensor is placed on top of a vibration generator at the sensor's jacket part to create a photo elastic effect that affects the power detected by the OPM [25]. The vibration generator is connected to an audio generator to produce reference vibrations in the form of mechanical waves at specific frequencies, which are validated using a digital oscilloscope. The sensor design is then calculated with vibrations at frequencies ranging from 3 Hz to 21 Hz with 3 Hz increments.

Data Acquisition

After the calibration process, the designed sensor is then tested to measure blood pressure by interpreting mechanical vibrations at the pulse points of the brachial artery and radial artery [26], as illustrated in Figure 5. By measuring at two different arterial locations, the results can be evaluated to determine the accuracy and consistency of the optical Fiber sensor in various conditions and body positions.

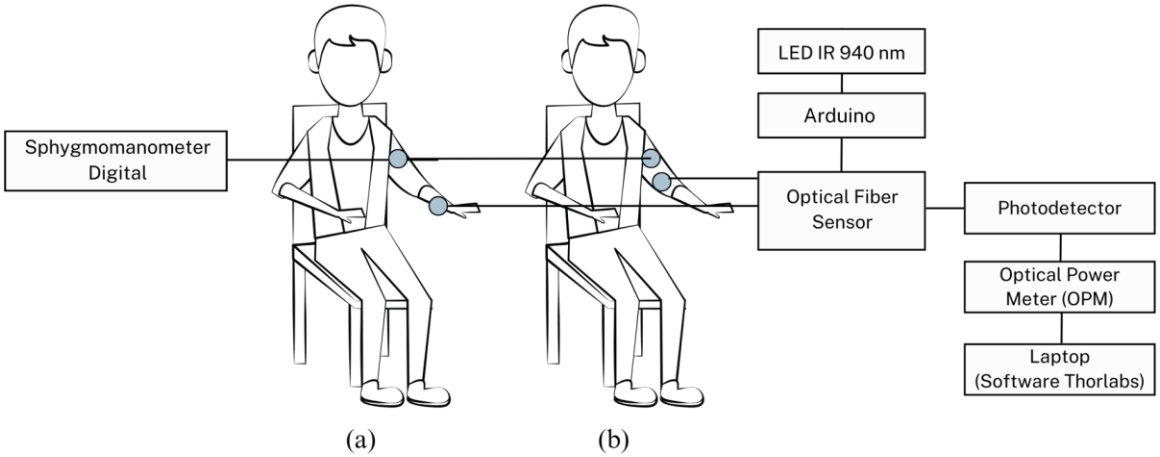

Figure 5. Setup for blood pressure data acquisition using optical fiber sensor and digital sphygmomanometer (a) radial artery. (b) brachial artery.

Data collection on the brachialis artery and radialis artery was carried out on the subjects in a relaxed position and condition, the arm position adjusted to the height of the heart. The subject is a man 21 years old. Before data recording, the BMI value of the subject is calculated first so that the subject is in the criteria with a normal BMI. In Figure 5, data recording on the sensor is performed for 120 seconds with 5 repetitions in every location and is conducted simultaneously with the SICHENYOU brand digital sphygmomanometer, which has a measurement accuracy of ± 3mmHg/plus 0.4kPa (blood pressure) ± 5% (pulse rate).

Signal Conditioning

The physical quantities generated by the designed optical Fiber sensor can be read by the OPM connected to a PC as a power difference in dBm over seconds through Origin software. The analog signal in the calibration process is filtered using a band-pass filter with a cut-off frequency of 2-22 Hz, smoothed, and transformed into the frequency domain using FFT. For test data on subjects, a band-pass filter with a cut-off frequency range of 0.5-1.5 Hz is used, which matches the normal arterial wave frequency of around 0.5-5 Hz. Smoothing is performed using the Adjacent-Averaging method. The estimated values of systolic blood pressure (SBP) and diastolic blood pressure (DBP) are obtained from the pulse transit time (PTT) [13], [14], [15], [27]. values with equations (1) and (2).

$$SBP = K_a \ln(PTT) + K_b \frac{1}{PTT^2} + K_c \quad (1)$$

$$DBP = Y_a \ln(PTT) + Y_b \frac{1}{PTT^2} + Y_c \quad (2)$$

Where K_a, K_b, K_c, Y_a, Y_b, and Y_c are coefficients related to the individual, which can be obtained through the calibration of a large sample data set from the blood pressure monitor. The Nonlinear Least Squares method is used for PTT-BP curve fitting [17].

Data Processing

In this study, 70% of the PTT data was used for model fitting, while the remaining 30% was used for testing. The coefficients in equations (1) and (2) were calculated using MATLAB, with the fitting results explained in Table 1.

Table 1. Curve fitting coefficients

Coefficients	Coefficient Values
Ka	-151.488
Kb	-48.418
Kc	146.6401
Ya	369.1508
Yb	149.8086
Yc	-81.0986

The coefficients in Table 1 are used in mathematical modelling to estimate blood pressure values based on the measured PTT values. The modelling equations are explained in equations (3) and (4).

$$SBP = -151.4880\, ln(PTT) - 48.4180 \frac{1}{PTT^2} + 146.6401 \quad (3)$$

$$DBP = 369.1508\, ln(PTT) + 149.8086 \frac{1}{PTT^2} - 81.0986 \quad (4)$$

Evaluation of the estimation model was performed using the Mean Absolute Error (MAE) method with equation (5).

$$MAE = \frac{1}{n}\sum_{i=1}^{n}|y_i - \hat{y}_i| \quad (5)$$

where n is the number of samples or data points, yi is the actual value of the -i data point, and $\hat{y}i$ is the predicted value of the -i data point. The smaller the MAE value, the better the model in predicting the actual values

$$Accuracy = (1 - \frac{MAE}{mean(y)} \times 100\%) \quad (6)$$

where mean(y) is the average value of the reference values.

Sensor Validation

A comparative analysis of systolic blood pressure (SBP) and diastolic blood pressure (DBP) values over one cardiac activity cycle between the designed optical Fiber sensor and the sphygmomanometer was conducted to evaluate the consistency and accuracy of the results

obtained. This validation aims to ensure that the optical Fiber sensor can provide comparable and reliable blood pressure measurement results.

Results and Discussion

The optical fiber sensor designed in this study has been used to measure blood pressure with various configurations illustrated in Figure 6.

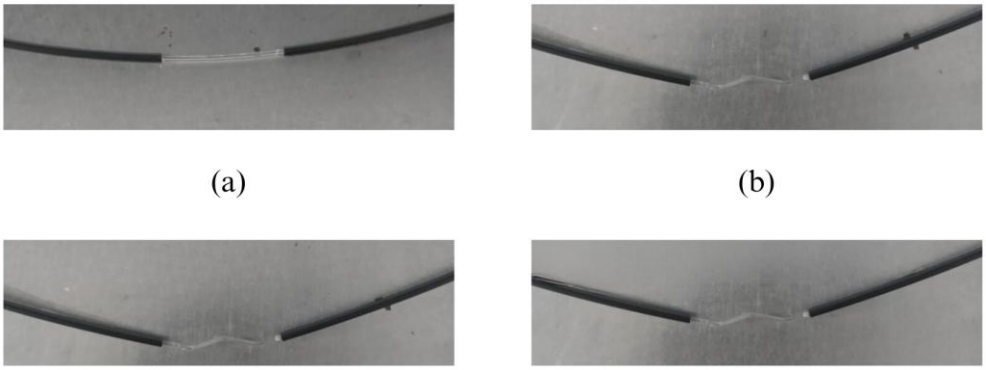

Figure 6. POF sensor configuration (a) Straight Configuration – 3 Scratches. (b) Bend Configuration. (c) Bend Configuration – 1 Scratch. (d) Bend Configuration – 3 Scratches

The configurations in Figure 6 differ in the sensing area, where light loss occurs due to bending or scratching on the fiber, resulting in changes in input power and output power detected by the detector. Bending and scratching the fiber are done to increase the sensor's sensitivity to detect small changes due to pressure or vibrations from the arterial pulse wave. A straight configuration with 3 scratches is used to see if signal detection remains effective without bending. Variations in the number of scratches in the bending configuration were performed to evaluate whether the combination of bending, and the number of scratches significantly affected the sensitivity of the sensor, so that the most optimal sensor configuration could be found in detecting small pressure changes that occurred in arterial pulse waves.

Calibration Results

The optical fiber sensor designed with the bend configuration can detect the input signal by producing a sinusoidal signal, indicating that the sensor can detect vibrations from the vibration generator. The calibration signal is illustrated in Figure 7.

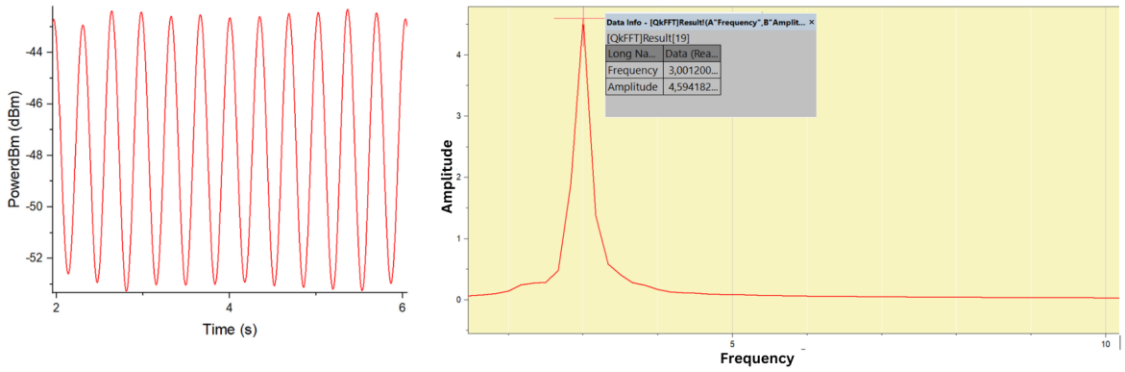

(a) (b)

Figure 7. (a) Calibration results graph after filtering, (b) Signal frequency spectrum after FFT

In Figure 7, the highest peak in the FFT magnitude spectrum represents the dominant frequency component in the signal. This peak is at a frequency close to the reference frequency value, indicating that the sensor can effectively respond to the specified frequency, and the band-pass filter successfully eliminates frequencies outside the cut-off range. The linear relationship between source frequency and the detected power was analyzed using the linear regression method. The linearity graph between the power detected by the plastic optical fiber sensor and the reference frequency is explained in Figure 8.

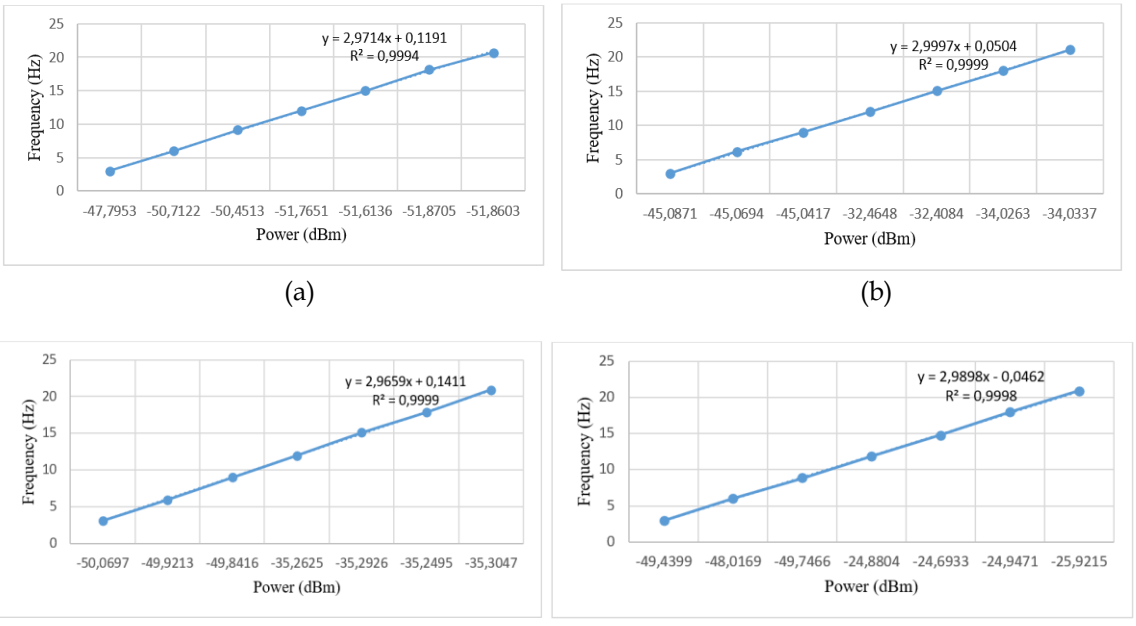

(a) (b)

(c) (d)

Figure 8. Linearity Graph (a) Bend Configuration (b) Bend Configuration – 1 Scratch (c) Bend Configuration – 3 Scratches (d) Straight Configuration – 3 Scratches

The linearity graphs in Figure 8 show that the sensor in each configuration exhibits linearity, marked by a linearity equation with a slope representing the sensor's sensitivity. This sensitivity serves to assess the sensor's ability to respond to changes. Additionally, the static characteristics of each sensor configuration are explained in Table 2.

Table 2. Static characteristics and sensor configuration comparison

Sensor Configurations		MAE	Accuracy (%)	Linearity	Sensitivity (Hz/dBm)
Bend		0.233	99.767	0.9994	2.9714
Bend – 1 Scratch	√	0.1564	99.8436	0.9999	2.9997
Bend – 3 Scratches		0.2804	99.7196	0.9999	2.9659
Straight – 3 Scratches		0.2801	99.7199	0.9998	2.9898

From Table 2, the bend configuration – 1 scratch shows the best overall performance with the lowest error value and the highest linearity, accuracy, and sensitivity. This indicates that the plastic optical fiber sensor with the bend configuration – 1 scratch is the best sensor configuration for the measurements performed.

Blood Pressure Data Collection

Data collection was conducted at the pulse points of the brachial artery and radial artery. The brachial artery and radial artery are among the most accessible areas for blood pressure and heart rate/pulse rate sampling [13], [26]. This is because these arteries are located near the surface of the skin, allowing the sensor to detect changes more clearly and accurately. Measurements at both points allow verification of whether the sensor can consistently detect changes in different locations. The raw data collected were then processed using a band-pass filter with a frequency range of 0.5-1.5 Hz [27] to isolate the fundamental components of the arterial waveform, particularly the percussion and dicrotic waves [17], [18]. Which is adjusted to the normal arterial wave frequency which is 0.5-5 Hz. The results after the filtering process are presented in Figure 9.

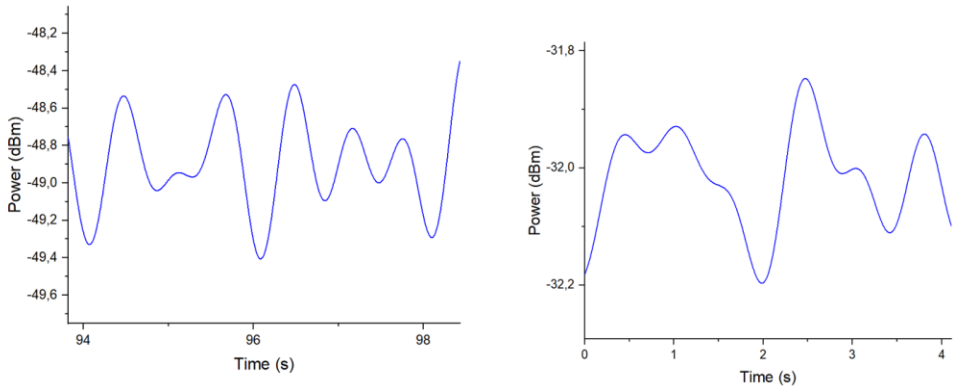

Figure 9. Filtering results using band-pass filters

After the filtering process, the acquired data were smoothed using the adjacent-averaging method to obtain the pattern of the arterial pulse wave detected by the plastic optical fiber sensor, as presented in Figure 10.

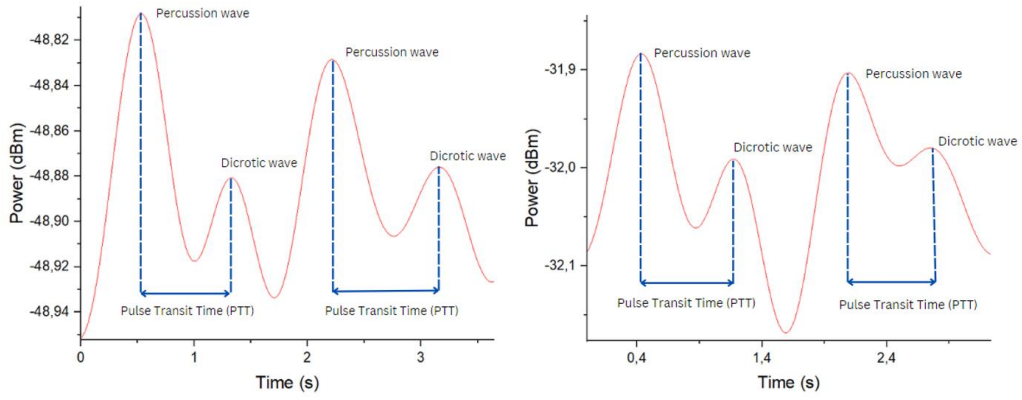

(a) (b)

Figure 10. Arterial pulse wave pattern from POF sensor after filtering and smoothing
(a) Bend Configuration – 1 Scratch on the radial artery
(b) Bend Configuration – 1 Scratch on the brachial artery

The results in Figure 10 show two peaks that can be identified as the percussion wave and the dicrotic wave. The percussion wave is the first peak in the arterial pulse signal caused by the contraction of the left ventricle of the heart as it pumps blood into the aorta and arteries. Meanwhile, the dicrotic wave is the second peak in the arterial pulse signal that occurs after the percussion wave, caused by the closure of the aortic valve, producing a reflected wave that moves back through the arteries. This indicates that the designed optical fiber sensor can detect the arterial pulse wave pattern. The performance evaluation of the plastic optical fiber sensor was based on the MAE and accuracy in measuring SBP and DBP compared to the digital sphygmomanometer. The MAE and accuracy results for the sensors at the radial and brachial locations are described in Table 3 and Table 4. The MAE values in both tables are used to calculate and evaluate the accuracy of each sensor configuration, which is explained in Table 5.

Table 3. Mean Absolute Error (MAE) and Sensor Accuracy in Radial

Sensor Locations		Sensor Configurations	MAE		Accuracy (%)	
			SBP	DBP	SBP	DBP
Radial		Bend	2.1544	3.4545	97.8669	95.0414
	√	**Bend with - 1 Scratch**	**1.7215**	**2.3981**	**98.2955**	**96.5577**
		Bend with - 3 Scratches	3.2432	7.6658	96.7889	88.9965
		Straight with - 3 Scratches	7.2029	16.3611	92.8685	76.5152

Table 4. Mean Absolute Error (MAE) and Sensor Accuracy in Brachial

Sensor Locations		Sensor Configurations	MAE		Accuracy (%)	
			SBP	DBP	SBP	DBP
Brachial		Bend	7.8805	16.9941	92.1975	75.6065
		Bend with - 1 Scratch	8.1493	24.7650	91.9314	64.4521
		Bend with - 3 Scratches	10.3921	34.8016	89.7108	50.0425
	√	**Straight with - 3 Scratches**	**2.8132**	**5.1066**	**97.2147**	**92.6699**

Based on the MAE and accuracy data in Tables 3 and 4, there are significant differences in the performance of various plastic optical fiber sensor configurations at different placement locations for measuring SBP and DBP. At the radial location, the Bend-1 Scratch configuration showed the best performance with the lowest MAE (1.7215 for SBP and 2.3981 for DBP) and the highest accuracy (98.2955% for SBP and 96.5577% for DBP). Meanwhile, at the brachial location, the Straight-3 Scratches configuration provided the best performance with the lowest MAE (2.8132 for SBP and 5.1066 for DBP) and the highest accuracy (97.2147% for SBP and 92.6699% for DBP). These results meet the British Hypertension Society standards, where blood pressure measurements are acceptable if they have an error of ± 5 mmHg for systolic and diastolic pressures [28]. To further strengthen performance claims of this study, a comparison of MAE of the proposed method with several previous studies has been made in Table 6.

Table 5. Comparison of different methodology in SBP and DBP measurement based on MAE.

No		Optical Sensor Method	MAE		Accuracy (%)		Ref.
			SBP	DBP	SBP	DBP	
1		FBG	3,5	2,8	-	-	[21]
2		BOTDA	4,2	3,0	-	-	[31]
3		MZI	2,8	2,1	-	-	[32]
4	√	**POF**	**1,72**	**2,39**	**98,2955**	**96,5577**	**[Author]**

As explained in Table 5, the POF method demonstrated exceptional performance in blood pressure measurement, with the lowest MAE values of 1.72 for SBP and 2.39 for DBP indicating minimal deviation from the true values. Additionally, the method achieved high accuracy rates of 98.2955% for SBP and 96.5577% for DBP, reflecting its excellent precision and reliability in detecting blood pressure changes. These results position the POF sensor as the most accurate and effective technique in comparison to other optical sensor methodologies, such as FBG, BOTDA, and MZI, which showed higher MAE values and lacked detailed accuracy data. Overall, the POF method stands out as a promising approach for non-invasive and precise blood pressure monitoring in clinical and research settings.

Overall, the optimal sensor configuration varies depending on the anatomical and physiological characteristics of the exact placement location and how the scratches on the optical fiber affect optical loss and the sensor's sensitivity to the vibrations produced by the pulse, thereby obtaining accurate blood pressure measurements.

Conclusion

Plastic optical fiber sensors have been successfully developed for a blood pressure measurement system with a sensing area of 3 cm and various sensor configurations, namely Bend, Bend with 1 Scratch, Bend with 3 Scratches, and Straight with 3 Scratches. Testing was conducted at two body locations, the radial artery and brachial artery. This optical fiber sensor demonstrated good static characteristics in terms of error, accuracy, linearity, and sensitivity. The Bend configuration – 1 Scratch showed the best performance with an error value of 0.1564, an accuracy of 99.8436%, a linearity of 0.9999, and a sensitivity of 2.9997. In the radial artery test, the Bend configuration – 1 Scratch provided the best results with the lowest MAE (1.7215 for SBP and 2.3981 for DBP) and the highest accuracy (98.2955% for SBP and 96.5577% for DBP). Meanwhile, in the brachial artery test, the Straight configuration – 3 Scratches showed the best performance with the lowest MAE (2.8132 for SBP and 5.1066 for DBP) and the highest accuracy (97.2147% for SBP and 92.6699% for DBP).

Acknowledgment

We would like to express our gratitude for the contributions, support, and assistance provided by various parties in this research, especially the dissertation supervisor and colleagues at the ITS Photonics and UNAIR Instrumentation Laboratories.

References

[1] D. Aune, Y. Mahamat-Saleh, E. Kobeissi, T. Feng, A. K. Heath, and I. Janszky, "Blood pressure, hypertension and the risk of atrial fibrillation: A systematic review and meta-analysis of cohort studies," *Eur J Epidemiol*, vol. 38, no. 2, pp. 145–178, Feb. 2023.

[2] R. Singh and others, "Hypertension and stroke in Asia: Prevalence, control and strategies in developing countries for prevention," *J Hum Hypertens*, vol. 14, no. 10–11, pp. 749–763, Oct. 2000.

[3] L. Minna, B. Ferdinando, C. Ronald, G. Richard, J. Jared, and N. Mingming, "Electronic diary monitoring for hypertension post stroke," *Journal of Hypertension Management*, vol. 9, no. 1, p. 73, Jun. 2023.

[4] S. S. Franklin and N. D. Wong, "Hypertension and cardiovascular disease: Contributions of the Framingham heart study," *Glob Heart*, vol. 8, no. 1, pp. 49–57, Mar. 2013.

[5] I. N. Wirakhmi and D. Novitasari, "Pemberdayaan Kader Pengendalian Hipertensi," *Jurnal Altifani Penelitian dan Pengabdian Kepada Masyarakat*, vol. 1, no. 2, pp. 240–248, 2021, doi: 10.25008/altifani. v1i3.162.

[6] American Heart Association (AHA), "Understanding Blood Pressure Reading," 2022. [Online]. Available: https://www.heart.org/en/health-topics/high-blood-pressure/understanding-blood-pressure-readings

[7] World Health Organization (WHO), "Hypertension," 2023. [Online]. Available: https://www.who.int/news-room/fact-sheets/detail/hypertension

[8] Kementerian Kesehatan Republik Indonesia (Kemenkes RI), "Hipertensi Penyakit Paling Banyak Diidap Masyarakat," 2019. [Online]. Available: https://www.kemkes.go.id/article/view/19051700002/hipertensi-penyakit-paling-banyak-diidap-masyarakat.html

[9] C. Goodman and G. Kitchen, "Measuring Arterial Blood Pressure," *Anaesthesia & Intensive Care Medicine*, vol. 22, pp. 49–53, 2021.

[10] L. Maharani, "Implementasi Pengukuran dan Klasifikasi Tekanan Darah Berdasarkan Pulse Transit Time Menggunakan Metode Transformasi Wavelet dan Support Vector Machines," 2016.

[11] B. S. Alpert, D. Quinn, and D. Gallick, "Oscillometric blood pressure: A review for clinicians," *Journal of the American Society of Hypertension*, vol. 8, no. 12, pp. 930–938, Dec. 2014.

[12] C. F. Babbs, "The origin of Korotkoff sounds and the accuracy of auscultatory blood pressure measurements," *Journal of the American Society of Hypertension*, vol. 9, no. 12, pp. 935–950, Dec. 2015.

[13] C. Qiu, T. Wu, F. Heydari, J.-M. Redouté, and M. R. Yuce, "Wearable blood pressure monitoring based on bio-impedance and photoplethysmography sensors on the arm," in *Proceedings of IEEE SENSORS*, Oct. 2018, pp. 1–3.

[14] S. Hoshide and others, "Pulse transit time-estimated blood pressure: A comparison of beat-to-beat and intermittent measurement," *Hypertension Research*, vol. 45, no. 6, pp. 1001–1007, Jun. 2022.

[15] S. Rao, K. Adithi, and S. C. Bangera, "An experimental investigation on pulse transit time and pulse arrival time using ECG, pressure and PPG sensors," *Medical Novel Technologies and Devices*, vol. 17, Mar. 2023.

[16] S. Mehta, N. Kwatra, M. Jain, and D. McDuff, "Can't take the pressure? Examining the challenges of blood pressure estimation via pulse wave analysis," *arXiv preprint arXiv:2304.14916*, 2023.

[17] L. Li, Y. Li, L. Yang, F. Fang, Z. Yan, and Q. Sun, "Continuous and Accurate Blood Pressure Monitoring Based on Wearable Optical Fiber Wristband," *IEEE Sens J*, vol. 21, no. 3, pp. 2642–2650, 2021.

[18] Z. B. Zhou *et al.*, "Wearable Continuous Blood Pressure Monitoring Devices Based on Pulse Wave Transit Time and Pulse Arrival Time: A Review," Mar. 01, 2023, *MDPI*. doi: 10.3390/ma16062133.

[19] S. Rizkiyah, "Perancangan Sensor Beban Menggunakan Serat Optik Berstruktur Multimmode-Singlemode-Multimode (MSM) untuk Sistem Weight In Motion (WIM)," 2016.

[20] A. K. Arifin, M. Lebang, S. Yunus, I. Dewang, I. Idris, and D. Tahir, "Measurement heart rate based on plastic optical fiber sensor," in *Journal of Physics: Conference Series*, Institute of Physics Publishing, May 2019, p. 12074. doi: 10.1088/1742-6596/1170/1/012074.

[21] S. H. Mardiyati, "Measurement of Blood Pressure Using Fiber Bragg Grating Sensor," *IEEE Sens J*, vol. 17, no. 5, pp. 1527–1532, 2017.

[22] S. Chino, H. Ishizawa, S. Koyama, and K. Fujimoto, "Influence of Installing Method on Pulse Wave Signal in Blood Pressure Prediction by FBG Sensor," in *2018 IEEE International Symposium on Medical Measurements and Applications (MeMeA)*, IEEE, Jun. 2018, pp. 1–6. doi: 10.1109/MeMeA.2018.8438626.

[23] Y. Haseda, J. Bonefacino, H. Y. Tam, S. Chino, S. Koyama, and H. Ishizawa, "Measurement of pulse wave signals and blood pressure by a plastic optical fiber FBG sensor," *Sensors*, vol. 19, no. 23, Dec. 2019, doi: 10.3390/s19235088.

[24] J. Bonefacino and others, "Ultra-fast polymer optical fibre Bragg grating inscription for medical devices," *Light Sci Appl*, vol. 7, no. 3, p. 17161, Mar. 2018, doi: 10.1038/lsa.2017.161.

[25] M. F. Farobi, "Rancang Bangun Balistokardiograf Berbasis Sensor Serat Optik Singlemode-Multimode-Singlemode (SMS)," 2023.

[26] C. P. Mayoral, "Fiber Optic Sensors for Vital Signs Monitoring: A Review of Its Practicality in the Health Field," *Biosensors (Basel)*, vol. 11, no. 2, p. 58, 2021.
[27] Y.-H. Kao, "Towards maximizing the sensing accuracy of an cuffless, optical blood pressure sensor using a high-order front-end filter," *Microsystem Technologies*, vol. 24, no. 11, pp. 4621–4630, 2018.
[28] British Hypertension Society (BHS), "Guidelines for management of hypertension," 2004.
[29] Widianto, A. A., Romdhoni, M. F., Karita, D., & Purbowati, M. R.. Hubungan Pola Makan dan Gaya Hidup Dengan Angka Kejadian Hipertensi Pralansia dan Lansia di Wilayah Kerja Puskesmas I Kembaran. Junal Unimus, Vol. 1 No.5, 2018.
[30] C. Peng, M. Chen, H. K. Sim, Y. Zhu, and X. Jiang. "Non-invasive and nonocclusive blood pressure monitoring via a flexible piezo-composite ultrasonic sensor," IEEE Sensors J., vol. 21, no. 3, pp. 2642–2650, Feb. 2021.
[31] X. Li (2019) Continuous Blood Pressure Monitoring Using Brillouin Optical Time-Domain Analysis. Optics Express, vol. 27, no. 3, pp. 2863-2875
[32] T. Nguyen. (2021). Blood Pressure Estimation Using Mach-Zehnder Interferometer Based Fiber Optic Sensor. Biomedical Optics Express, vol. 12, no. 4, pp. 1789-1798